Molecular structure and intramolecular hydrogen bond strength of 3-methyl-4-amino-3-penten-2-one and its N-Me and N-Ph substitutions by experimental and theoretical methods

Seyedkatouli , Seyedabdollah ; Vakili, Mohammad; Tayyari , Sayyed Faramarz ; Hansen, Poul Erik; Kamounah, Fadhil S.

Published in:
Journal of Molecular Structure: THEOCHEM

DOI:
10.1016/j.molstruc.2019.02.007

Publication date:
2019

Document Version
Peer reviewed version

Citation for published version (APA):
Seyedkatouli , S., Vakili, M., Tayyari , S. F., Hansen, P. E., & Kamounah, F. S. (2019). Molecular structure and intramolecular hydrogen bond strength of 3-methyl-4-amino-3-penten-2-one and its N-Me and N-Ph substitutions by experimental and theoretical methods. *Journal of Molecular Structure: THEOCHEM*, *1184*, 233-245. https://doi.org/10.1016/j.molstruc.2019.02.007

Accepted Manuscript

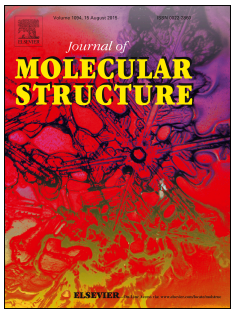

Molecular structure and intramolecular hydrogen bond strength of 3-methyl-4-amino-3-penten-2-one and its N—Me and N-Ph substitutions by experimental and theoretical methods

Seyedabdollah Seyedkatouli, Mohammad Vakili, Sayyed Faramarz Tayyari, Poul Erik Hansen, Fadhil S. Kamounah

PII: S0022-2860(19)30131-0

DOI: https://doi.org/10.1016/j.molstruc.2019.02.007

Reference: MOLSTR 26164

To appear in: *Journal of Molecular Structure*

Received Date: 10 November 2018

Revised Date: 2 February 2019

Accepted Date: 4 February 2019

Please cite this article as: S. Seyedkatouli, M. Vakili, S.F. Tayyari, P.E. Hansen, F.S. Kamounah, Molecular structure and intramolecular hydrogen bond strength of 3-methyl-4-amino-3-penten-2-one and its N—Me and N-Ph substitutions by experimental and theoretical methods, *Journal of Molecular Structure* (2019), doi: https://doi.org/10.1016/j.molstruc.2019.02.007.

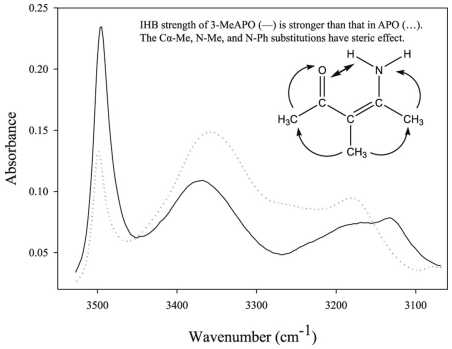

Molecular structure and intramolecular hydrogen bond strength of 3-methyl-4-amino-3-penten-2-one and its N-Me and N-Ph substitutions by experimental and theoretical methods.

Seyedabdollah Seyedkatouli [a], Mohammad Vakili [* a], Sayyed Faramarz Tayyari [a], Poul Erik Hansen [b], Fadhil S. Kamounah [c]

[a] Department of Chemistry, Faculty of science, Ferdowsi University of Mashhad, Mashhad 91775-1436, Iran.

[b] Department of Science and Environment, Roskilde University, Universitetsvej 1, P.O. Box 260, DK-4000 Roskilde, Denmark.

[c] Department of Chemistry, University of Copenhagen, Universitetsparken 5, DK-2100, Copenhagen Ø, Denmark.

Abstract

In the present work, molecular structures and intramolecular hydrogen bonding (IHB) of 3-methyl-4-amino-3-penten-2-one, 3-MeAPO, 3-methyl-4-methylamino-3-penten-2-one, 3-Me-MeAPO, and the 3-methyl-4-phenylamino-3-penten-2-one, 3-Me-PhAPO have been investigated by means of density functional theory (DFT) calculations, at the B3LYP/6-311++G** level, and experimental investigations including NMR, IR, Raman, UV spectroscopy, and X-ray crystallographic methods. The mentioned results were compared to those of 4-amino-3-penten-2-one, APO. DFT calculations suggest a relatively strong intramolecular hydrogen bond in 3-MeAPO and its N-Me and N-Ph substituted derivatives with N···O distances of 2.597, 2.584, and 2.581 Å, and calculated hydrogen bond energies of about 10.9, 13.6, and 14.9 kcal/mol in 3-MeAPO, 3-Me-MeAPO, and 3-Me-PhAPO, respectively. While, the calculated N···O distances and hydrogen bond energies, of APO, 2.669 Å and 7.67 kcal/mol respectively, suggest a medium IHB strength. According to the NBO results, the steric effect is the dominant factor for changes of the IHBs. The calculated geometrical parameters of 3-MeAPO are in excellent agreement with

* Corresponding author. Tel.: +98 9153215410;

E-mail address: vakili-m@um.ac.ir (M. Vakili).

the X-ray results. UV-Vis spectra of 3-MeAPO, 3-Me-PhAPO, and 3-Me-MeAPO were recorded in ethanol supporting the results mentioned above. According to the calculated results and deuterium isotope effects on ^{13}C chemical shifts, 3-MeAPO exists as a keto-amine. Comparison of the observed and theoretical IR and Raman spectra and the spectral behavior upon deuteration were used for assignment of the vibrational spectra of 3-MeAPO. The assigned normal modes were compared to those of APO. The theoretical results were in good agreement with the experimental data. The vibrational frequencies also confirmed that the IHB strength in 3-MeAPO is stronger than that in APO.

Keywords: 3-methyl-4-amino-3-penten-2-one; Substitution effect; Intramolecular hydrogen bond; Molecular spectroscopy; Isotope effects on ^{13}C chemical shifts.

1. Introduction

α,β-Unsaturated-β-ketoenamines, also known as β-ketoenamines, are important organic chemicals for synthesis of an assortment of heterocyclic and medical compounds [1-4]. α,β-Unsaturated-β-ketoenamines have in many cases been shown to exist at the aminoketone form [5-14], whereas *o*-hydroxy Schiff bases can be tautomeric [15, 16]. In the present case the steric repulsion may reduce the N…O distance and lead to tautomerism. The compounds can in principle exist as three different tautomers in equilibrium, i.e., iminoketone, aminoketone, and iminoenols, see Fig. 1. The aminoketone forms are usually more stable than the iminoenol forms, which are the major form of β-enaminones [8-10, 12]. Hydrogen bonding is one of the most important of all inter- and intramolecular interactions. The hydrogen bond plays an essential role in phenomena such as crystal engineering, stabilization of the secondary structure of biomolecules like proteins, and DNA [17-20]. The formation of an IHB leads to an increase of the resonance conjugation of the π-electrons in the chelated ring. Any factor which effects this resonance, can change the IHB strength. Synthesis, IR, and NMR spectra of some α,β-unsaturated-β-ketoenamines have been already reported [5, 14, 21-25].

The study of IHB strength in 3-MeAPO, with a methyl group in the α-position could be interesting. In addition, in 3-Me-MeAPO and 3-Me-PhAPO, with a methyl as bulky group or a phenyl group as electron donating group on the nitrogen atom could influence the IHB strength.

Therefore, comparison of IHB strength with APO may increase our insights into the effects of these substitutions on the IHB strength.

The structure, vibrational assignment, and IHB strength of the title molecules, theoretically and experimentally, were not reported previously. In addition, the aim of the present study is to investigate tautomerism, conformations (3-MeAPO is special with its three interlocking methyl rotamers), molecular structure, spectroscopic analysis, and the IHB strength of title molecules, by different theoretical and experimental approaches. The theoretical (such as the optimized configuration, the geometric parameters, simulating vibrational spectra, UV spectra, and ^{1}H and ^{13}C NMR chemical shifts, NBO, and atoms in molecules (AIM) [26] analysis) and experimental results (including IR, Raman, NMR, and UV-Vis spectra) for the title molecules have been compared with the corresponding data for 4-amino-3-penten-2-one (APO), as the simplest member of the β-enaminones compounds [27, 11]. In addition, we compared the mentioned theoretical and experimental results of N-Me and N-Ph substitutions with 3-Me-APO. These comparisons give a clear understanding of the substitution effects of "CH_3 and phenyl groups" in the α- and on the nitrogen positions on the IHB strength.

2. Experimental

2.1. Materials

3-Methyl-2, 4-pentanedione (3-Meacac) was purchased from Alfa Aesar. Other compounds and solvents were of analytical grades and used as received.

4-Amino-3-penten-2-one (3-MeAPO):

This compound was prepared according to a procedure similar to that described for APO [28]. In a 25 ml round bottom flask, 3-Meacac (2.28 g, 20 mmol) was charged and cooled in the ice bath with stirring and 25% of ammonia solution (3.5 ml) was added dropwise, immediate white precipitation developed. After complete addition, the mixture was left stirred at room temperature for 30 minutes and left stand in a stoppered flask for 48 h. The solid was treated with diethyl ether (75 ml) and washed with distilled water (2x75 ml) and brine (75 ml). The organic portion was separated and dried with anhydrous sodium sulfate. Evaporation of ether under reduced pressure yields a white solid. Recrystallization from n-heptane/ethyl acetate gave colorless needles (1.85 g, 82%), m.p. 111.5-112.0 °C, lit. 109-110 °C [29].

4-(Methylamino)-3-penten-2-one (*3-Me-MeAPO*):

This compound was synthesized by modification of a literature method [30, 31]. To a solution of α-methyl acetylacetone (1.23 g, 11.0 mmol) in absolute ethyl alcohol (10 ml) was added a 2M solution of methylamine in THF (10 ml, 20 mmol) and the clear solution was stirred at room temperature in a stoppered flask for 15 hrs. The volatile solvents were evaporated under reduced pressure and the light amber oil residue was purified by flash column chromatography on silica gel using n-heptane/ethyl acetate (2:1) to obtain the desired pure product as a pale amber oil which solidified on cooling 1.12 g (82% yield).

4-(Phenylamino)-3-methyl-3-penten-2-one (3-Me-PhAPO):

To a solution of α-methyl acetylacetone (2.28 g, 20.0 mmol) in methanol (25 ml) was added aniline (1.86 g, 20.0 mmol) at room temperature, followed by concentrated formic acid (3 drops). The mixture was stirred at room temperature for 15 minutes, then refluxed under a nitrogen atmosphere for 15 hrs. Methanol was evaporated under reduced pressure and the yellow oil residue was chromatographed on silica gel, using n- heptane/ethyl acetate (10:1) and (1:2) to obtain the pure compound as an amber oil, which solidified on cooling 3.40 g (90% yield).

The deuterated analogues for the IR studies, include D_2-3-MeAPO, D-3-Me-PhAPO, and D-3-Me-MeAPO, were prepared by the following procedure [32]. 0.5 g of the under-study molecules was dissolved in CCl_4 (3 ml) and a drop of triethylamine was added and stirred for an hour. Then, D_2O (1 mL) was added and the mixture stirred for 24 h. The CCl_4 solutions were separated and dried over anhydrous Na_2SO_4. Solid D_2-3-MeAPO was obtained by removing the solvent in a vacuum desiccator. The IR and Raman spectra confirmed that the hydrogen atoms of amino group were more than 90% replaced by deuterium atoms.

The partially deuterated compounds for the isotope effect on chemical shift studies were obtained by dissolving the compounds in CH_3OD:CH_3OH and evaporating off the solvent under reduced pressure.

2.2. Instrumentation

The NMR spectra were recorded on an Avance Bruker-400 MHz spectrometer. All chemical shifts are reported relative to TMS, using 2 mol% solutions in $CDCl_3$ at 22ºC. For 3-APO ^{1}H NMR ($CDCl_3$): δ 10.32 (br, NH_{in}), 5.30 (br, NH_{out}), 2.08 (s, H(CH_3-C=O)), 1.93(s, H(CH_3-C-N)), 1.78(s, H(CH_3-Cα) and for ^{13}CNMR: δ 197.35 (C2), 158.94 (C4), 99.01 (C3),

28.56 (C1), 21.86 (C5), 14.40 (C8). For APO: ^{1}H NMR ($CDCl_3$): δ 9.71 (br NH_{in}), 5.71 (NH_{out}), 5.03 (CH), 2.03 (CH_3) and 1.91 (CH_3). ^{13}C NMR: δ 196.69 (C2); 160.98 (C4); 95.75 (C3); 29.29 (C1); 22.25 (C5).

For 3-Me-MeAPO: ^{1}HNMR ($CDCl_3$): δ 1.78 (s, 3H, CH_3-Cα), 1.91 (s, 3H, CH_3-C-N), 2.06 (s, 3H, CH_3-C=O), 2.87 (d, 3H, CH_3-N, J=5.0), and 11.80 (b, 1H, NH bonded). The mentioned results are close to those reported results by Mikysek et al. [31]. ^{13}CNMR: δ 194.09 (C2), 162.89 (C4), 97.72 (C3), 29.59 (C1), 28.06 (C10), 14.68 (C8), and 14.58 (C5).

For 3-Me-PhAPO: ^{1}H NMR ($CDCl_3$): 1.91 (s, 3H, CH_3-Cα), 2.01 (s, 3H, CH_3-C-N), 2.21 (s, 3H, CH_3-C=O), 7.04 (d, 2H), 7.14 (t, 1H), 7.31 (t, 2H), δ 13.46 (br NH bonded). ^{13}C NMR: δ 196.43 (C2), 158.23 (C4), 139.35 (C10), 128.90 (C11, C13, and C15), 124.99 (C12 and C14), 100.87 (C3), 28.54 (C1), 16.95 (C5), and 14.76 (C8), which is good agreement with those reported by Xiang Chen et al. [23].

The ^{13}C NMR spectra for isotope effect measurements of APO and 3-MeAPO were recorded at 273K and data are given in Scheme1.

The ultraviolet absorption spectra were examined in the range of 200-400 nm at 298 K, using a Perkin Elmer LAMBDA 25 spectrophotometer. The UV–Vis spectrum of 3-MeAPO, 3-Me-MeAPO, and 3-Me-PhAPO were measured in ethanol solution.

The IR spectra in the region 4000–500 cm^{-1} were recorded on a Bomem MB-154 Fourier transform spectrophotometer using KBr pellets and CCl_4 solution. The spectra were collected with a resolution of 2 cm^{-1} by signal averaging of 20 scans.

The Far-IR spectra in the region 600–200 cm^{-1} were obtained using a Thermo Nicolet NEXUS 870 FT-IR spectrometer equipped with a DTGS/polyethylene detector and a solid substrate beam splitter with use of polyethylene disks. The spectrum was collected using CsI pellets with a resolution of 2 cm^{-1} by signal averaging the results of 32 scans.

The FT-Raman spectra in the region 3200–200 cm^{-1} were recorded employing a 180° backscattering geometry and a Bomem MB-154 Fourier transform Raman spectrometer. The instrument was equipped with a ZnSe beam splitter and a TE cooled In GaAs detector. The excitation wavelength at 1064 nm was obtained from a Nd/YAG laser. Rayleigh filtration was afforded by a set of two holographic technology filters. The spectra were accumulated for 8000 scans with a resolution of 2 cm^{-1}. The laser power at the sample was 500 mW.

2.3. Single crystal X-ray measurements

Single crystals of $C_6H_{11}NO$ were obtained by recrystallization from heptane/ethyl acetate as solvent. A suitable crystal was selected, and the crystal structure analysis was performed on a 'Bruker APEX-II CCD' diffractometer. The crystal was kept at 120 K during data collection. Using Olex2 [33], the structure was solved with the olex2.solve [34] structure solution program using Charge Flipping and refined with the ShelXL [35] refinement package using Least Squares minimization.

The crystallographic data and the details of the X-ray analysis are represented in Table S1. According to the X-ray results, the obtained unit cell dimensions are (7.916(4) × 9.438(4) × 8.951(4) Å). The other crystal data are: $C_6H_{11}NO$, M_r = 113.16, monoclinic, α = 90°, β = 104.308(17)°, γ = 90°, V = 648.0(5)Å^3, T = 120 K, Z = 4, 7239 reflections measured, Independent reflections=1483[R_{int}=0.0264, R_{sigma}=0.0195], final R indexes [I>=2σ (I)] R_1= 0.0391, wR_2 = 0.1046, final R indexes [all data] R_1 = 0.0463, wR_2 = 0.1097.

The selected calculated and observed bond lengths, bond angles, and dihedral angles for this compound are given in Table 1, and the X-ray and calculated structures for 3-MeAPO are shown in Fig. 2a-b. For comparison, the optimized structure of 3-Me-MeAPO and 3-Me-PhAPO are shown in this figure, Fig. 2c-d and tabulated in Table 1. The fractional atomic coordinates and anisotropic Displacement Parameters for heavy atoms are given in Tables S2 and S3, respectively. The fractional atomic coordinates for hydrogen atoms are listed in Table S4.

3. Method of analysis

Computations study have been carried out with the Gaussian 09 [36], AIM 2000 [37], and NBO 5.0 [38] software packages. The calculated total electronic energies, relative stabilities of all conformers of aminoketone, and iminoenol tautomers, and the calculated harmonic frequencies of aminoketone form of 3-MeAPO, were determined at the B3LYP level [39, 40] using the 6-311++G** basis set. In adittion, the molecular geometry and vibrational frequencies of 3-Me-MeAPO and 3-Me-PhAPO were calculated at the same level of theory. The assignments of observed wavenumbers were aided by the animation option of the Gauss View 4.1.2 graphical interface [41], which gives a visual presentation of the shape of the vibrational modes.

The assignments of the experimental frequencies are based on the observed band frequencies and intensities changes in the infrared and Raman spectra of the deuterated species

and confirmed by establishing one to one correlation between observed and theoretically calculated frequencies.

Second order interaction energies (E^2) [42] and steric exchange energies [43] were performed at the B3LYP/6-311++G**level, using NBO 5.0 software.

The nuclear shieldings for the three forms of 3-Me-APO and aminoketone form of other molecules and tetramethylsilane (TMS) have been obtained using the gauge-including atomic orbital (GIAO) method [44, 45] at the B3LYP/6-311++G** level. Data are given in section 4. 4. 1 and in the supplementary material, as Tables S5-6. The predicted ^{1}H and ^{13}C chemical shifts are obtained in two ways. The first from equation $\delta = \sigma_0 - \sigma$, where δ is the chemical shift, σ is the nuclear shielding, and σ_0 is the nuclear shielding of TMS, and the second by using of the equations between the experimental ^{1}H and ^{13}C chemical shifts (δ_{exp}) and nuclear shielding (σ_{calc}) of 3-Me-APO. According to this method the predicted chemical shifts of 3-Me-MeAPO and 3-Me-PhAPO are close to the experimental chemical shifts results, see Table S6.

The excitation transitions for the most stable conformer, the aminoketone form, of 3-MeAPO, 3-Me-MeAPO, 3-Me-PhAPO, and APO were calculated at the time-dependent, TD-DFT, B3LYP/6-311++G** level of theory in ethanol solution by the SCRF-PCM method [46].

AIM 2000 software was applied to obtain the electron density (ρ) and Laplacian ($\nabla^2\rho$) of electron density at the hydrogen bond critical points (BCP), according to Bader's AIM theory [26] at the above level of theory.

4. Results and discussion

4.1. Molecular geometry

As mentioned in the introduction, α, β-unsaturated-β-ketoenamines can form a tautomeric equilibrium between iminoketone, aminoketone, and iminoenol forms (see Fig. 1). We considered all conformers of all possible tautomers for 3-MeAPO. According to our calculations, the relative energies for the iminoenol and iminoketone forms are 6.86 and 10.38 kcal/mol higher than that of the most stable tautomer, the aminoketone form.

From the theoretical point of view, by considering the rotation of methyl groups around the C-C bonds, include C4-C5, C3-C8, and C2-C1 bonds, 8 cis-enol forms can be drawn for the aminoketone form of 3-MeAPO. The structures of these conformers and their relative stabilities

calculated at the B3LYP/6-311++G** level are shown in supplementary material, as Fig. S1. Among these forms, only one of them (AK1) is stable, while all other forms under full optimization turn to the AK1. The methyl groups in the C1 and C5 positions of 3-Me-APO (see Figure 2) and 3-Me-PhAPO molecules are eclipsed in relation to each other, while in APO and 3-Me-MeAPO molecules they are staggered.

The fully optimized geometrical parameters of 3-MeAPO, 3-Me-APO, 3-Me-PhAPO, and 4-amino-3-penten-2-one, APO, at the B3LYP/6-311++G** are collected in Table 1 together with the corresponding experimental data of 3-Me-APO. The calculated geometrical parameters of 3-MeAPO are in excellent agreement with the X-ray results, nearly within the experimental error. According to this table, the calculated N…O distance in 3-Me-PhAPO, 3-Me-MeAPO, 3-MeAPO, and APO are 2.581, 2.584, 2.597, and 2.669Å, respectively. These values confirm that the trend of the IHB strength is:

3-Me-PhAPO > 3-Me-MeAPO > 3-MeAPO > APO (1)

This trend is confirmed by the changes in the theoretical structure parameters such as, the shortening and lengthening of O···H distance, and N-H bond, respectively, and increasing of the NHO bond angle. The reported N…O distances for N-H···O systems lie in the 2.48-2.76 Å range [13, 14]. According to Table 1 and comparison of 3-MeAPO with APO, substitution of the methyl group in the α-position reduces the N…O and O…H distances and increases the OHN bond angle and N-H bond length. These results could be attributed to the repulsion between methyl groups in the α and β positions, which pushes the methyl groups in the β positions toward oxygen and nitrogen atoms, while the C-N and C=O bond lengths in the chelated ring are almost the same as those in APO. Comparison of N···O and the other component of the chelated ring in 3-MeAPO with those in 3-Me-MeAPO and 3-Me-PhAPO shows that in addition to the steric effect of the α-methyl group, the methyl and phenyl groups on the nitrogen atom are also involved in steric interactions, see the NBO analysis section, which agrees with the previously reported by Hill and Roodt [47]. The steric effect causes the N···O distance to diminish. The N···O distance of 3-Me-PhAPO is shorter than that in 3-Me-MeAPO, so the IHB in the former is stronger than the latter, which agrees with the other theoretical results and our experimental results, see Intramolecular hydrogen bond Energy and Experimental studies sections. The dihedral angle between the phenyl and the chelated rings in 3-Me-PhAPO is 142.3º, so

increasing of IHB strength through the resonance of the phenyl group with the chelated rings is not effective.

As it is shown in Table 1, lengthening of C=C and C-C bonds in 3-MeAPO molecule in comparison with APO, could be attributed to the steric effect of α-CH_3 on C-C-C fragment of chelated ring and increasing of π-electron delocalization in this fragment. This result is in excellent agreement with the reported results for halogen-substituted acetylacetonates of boron difluoride and α-alkyl derivates of copper (II) acetylacetonate [48, 49]. This Table also shows that the C2-C1 and C4-C5 bond lengths in all molecules are longer than the corresponding bond lengths in APO.

4.2. Tautomerism

The fact that no hydrogens nor carbons have chemical shifts corresponding to C-3 of the iminoketone form rules this out. Furthermore, the good agreement between the calculated nuclear shieldings and the observed chemical shifts for the aminoketone form confirms this form to be the major one. The fact that the fit could not be improved by mixing in calculated data for the aminoenol form shows that no tautomerism is at play. In addition, this is confirmed by the finding of a large positive two-bond isotope effect at C-4 and the negative deuterium isotope effects at C-2 [5, 7]. This shows that the compound exist primarily at the aminoketone form as the presence of the iminoenol form would lead to the opposite trend.

4.3. Intramolecular hydrogen bond Energy

It has been debated whether steric compression can lead to a stronger hydrogen bond [50, 51]. Hydrogen bond energies have in several intramolecularly hydrogen bonded systems been determined by the hydrogen bond and out method originally was suggested for salicylaldehyde by Cuma, Scheiner, and Kar [52]. However, this method requires that no steric interactions occur in the out position. This method can of course not be used for primary amines as investigated in the present case. A more promising approach for primary amines is to calculate energies in the cis hydrogen bonded system and subtract the energy of the relevant trans compound as suggested by Jablonski et. al. [53]. However, this method is only well suited for aldehyde derivatives. Jablonski et al. managed to estimate a hydrogen bond energy for 3-aminopropenal of 6.35 or 5.28 kcal/mol using at the MP2 level with 6-31G** and 6-311++G** basis sets, respectively.

According to our calculations, performed at the B3LYP/6-311++G** level, the electron density at the bond critical point gave a value of 0.027. Using the Espinosa equation [54] a hydrogen bond energy of 6.35 kcal/mol is estimated, near to Jablonski's values [53]. The latter method was developed based on intermolecular hydrogen bonds. Furthermore, this method was also used by Afonin et. al. in the intramolecular hydrogen bond systems [55]. In addition, the AIM calculations were also performed on the other studied molecules and APO, see Table 1. The E_{HB} values, in the gas phase, are 14.91, 13.63, 10.85, and 7.67 kcal/mol, in 3-Me-PhAPO, 3-Me-MeAPO, 3-MeAPO, and APO, respectively using this method. Rozas et al. [56] reported that the sign of the Laplacian of the electron density at the bond critical point ($\nabla^2\rho$BCP) could characterize the strength of hydrogen bond strength. According to Table 1, in 3-Me-PhAPO, 3-Me-MeAPO, and 3-MeAPO, the $\nabla^2\rho$BCP´s are more negative than those in APO. Thus, these AIM results also confirm the trend (1) for IHB strength.

The deuterium isotope effects on ^{13}C chemical shifts have been used to estimate hydrogen bond strength [57] and has in enaminones given clear indications of steric compression [7]. The two-bond isotope effect on the C-4 chemicals shift for 3-APO is clearly larger than for APO (see Scheme 1) showing as also indicated by the NH chemical shifts (10.32 vs. 9.71 ppm) a stronger hydrogen bond in the former. Therefore, the IHB strength of 3-MeAPO increases compared to that of APO and 3-aminopropenal. This is in excellent agreement with the theoretical N…O distance. The mentioned value in 3-MeAPO, APO, and 3-aminopropenal, at the B3LYP/6-311++G**, is 2.597, 2.669, and 2.718 Å, respectively. The increasing of the IHB strength in 3-MeAPO and APO in comparison to that in 3-aminopropenal, seems to indicate that the steric compression leads to a higher hydrogen bond energy.

4.4. NBO analysis

4.4.1. Electron delocalization

The NBO calculations can be used to estimate the energy of interactions between donor and acceptor orbitals, for characterization of IHBs. In addition, the pairwise exchange energies between filled NBO's i and j, calculated by the NBO 5.0, show the steric effect of different substitutions. Table S7, see supplementary materials, lists some of the important calculated electron delocalization (E^2) between donor and acceptor orbitals of APO, 3-MeAPO, 3-Me-

MeAPO, and 3-Me-PhAPO molecules. According to our results for E^2, there is no significant difference between the results for the studied molecules, which means that the IHB strength is not affected by the conjugation of substituents with chelated ring. This result agrees with the calculated dihedral angle between the phenyl ring and the chelated ring, 142.3º.

The lp(2) O6→σ* (N-H) parameter, as one of the most important hyperconjugative interactions which is proportional to the IHB strength, gives values well correlated to the N…O distance and this is in agreement with the trend (1) for IHB strength of the mentioned molecules. The mentioned values for APO, 3-MeAPO, 3-Me-MeAPO, and 3-Me-PhAPO are 8.19, 11.25, 16.09, and 19.00 kcal/mol. These values also confirm the trend (1) for the IHB strength.

4.4.2. Steric effect

Since, the only difference between the studied molecules is the methyl group (in the α-position), CH_3, and phenyl groups on the nitrogen, we only consider the steric effect of these groups with the rest of the molecule. Table S8 shows the steric effects of the mentioned groups in the α position and on the nitrogen atom. The α-methyl group in these molecules increase the steric hinderance between methyl and the rest of molecule and confirms stronger IHB in α-methyl molecules in comparison with APO. In addition, there is no significant difference for the mentioned steric hinderance in 3-MeAPO, 3-Me-PhAPO, and 3-Me-MeAPO molecules. The summation of pairwise exchange energies, which is made by N-Ph ring, is more than that in the N-methyl group, so the IHBs in 3-Me-PhAPO is stronger than that in 3-Me-MeAPO. This result also confirms the trend (1). The summation of the mentioned rows for 3-Me-PhAPO and 3-Me-MeAPO are 33.1 and 29.5 kcal/mol, respectively. The value of repulsive interactions agrees with the shorting of N…O distance and the trend (1). These values are 10.70, 14.83, 18.82, and 20.55 kcal/mol for APO, 3-MeAPO, 3-Me-MeAPO, and 3-Me-PhAPO, respectively.

4.5. Experimental studies

4.5.1. NMR spectroscopy

The calculated ^{13}C and ^{1}H chemical shifts (δ) and isotropic nuclear shilding (σ_{iso}) for stable forms of the three tautomers of 3-Me-APO are also shown in Table S5. In addition, the measured and calculated ^{1}HNMR and ^{13}C-NMR chemical shifts of 3-MeAPO, 3-Me-PhAPO, and 3-Me-MeAPO, are also compared in Table S6. The ^{1}HNMR and ^{13}CNMR spectra of 3-Me-

PhAPO, 3-Me-MeAPO, and 3-MeAPO are shown in Fig. S2a-f, respectively. Deuterium isotope effects on ^{13}C chemical shifts are measured for 3-MeAPO and APO (Scheme 1). These are measured at 273 K as averaging was taken place at ambient temperature. The isotope effects due to the hydrogen bonded deuterium are much larger than those from the non-hydrogen bonded one [58]. As isotope effects are largest over two bonds, large effects are expected at C-4, in this case 0.29 ppm for 3-MeAPO and 0.21 ppm for APO. This also confirms the assignment of C-4 and by default C-3. For C-5 the isotope effect is over three bonds and typically 0.05 ppm [7]. In the present case slightly larger.

The relationship between the experimental ^{1}H and ^{13}C chemical shifts (δ_{exp}) and the GIAO (Gauge-Including Atomic Orbitals) nuclear shielding (σ_{calc}) are widely used to relate those two parameters. This relationship is usually linear and described by the following equation: $\delta_{exp} = a\ (\sigma_{calc}) + b$. The equations for 3-Me-APO are -1.0278X+32.099 (-1.0265X+182.18), and their R^2 are 0.9925 (0.9999), respectively. The equation and value for $^{13}CNMR$ are in parenthesis. According to the mentioned equations, the estimated $^{1}HNMR$ and $^{13}CNMR$ chemical shifts of 3-Me-MeAPO and 3-Me-PhAPO are near to the experimental value, see Table S6.

For ^{13}C chemical shifts of aminoketone form in 3-MeAPO, the standard deviation, SD, is 0.71 ppm. As regression coefficients (R^2) indicate, the agreement between the experimental and calculated data for this form is satisfactory for carbon-13 (R^2=0.9999) and for proton chemical shifts (R^2=0.9925 and SD=0.38 ppm). Consequently, an agreement between B3LYP/6-311++G**calculated results and experimental NMR data is demonstrated. This could not be improved by mixing in data for the iminoenol form. The SD and R^2 values for $^{1}HNMR$ of 3-Me-MeAPO are 0.50(0.40) and 0.9998(0.9901), respectively. The values for 3-Me-PhAPO are in parenthesis. The mentioned values for ^{13}C-NMR are 1.01(3.30) and 0.9999(0.9972). The calculated and experimental δOH (in CCl_4) of all molecules confirm the trend (1) in IHB strength.

Some discrepancies between the obtained $^{1}HNMR$ results for 3-MeAPO with those reported by Ostercamp [29] are attributed to the chemical shifts values of methyl groups and hydrogen atoms of amine group (H9 and H10). We assigned the higher chemical shift to the methyl group in the carbonyl side, while this was attributed by Ostercamp [29] to the methyl group in the amine side. The other discrepancies between our results and Ostercamp work [29], is related to the values of chemical shift of the H9 and H10, which the first one has not been

reported, while the chemical shift of H10 is about 2.4 ppm less than the obtained result (See Fig. S2a).

4.5.2. UV-Vis spectra and electronic properties

The experimental UV–vis spectra of 3-MeAPO, 3-Me-MeAPO, and 3-Me-PhAPO, in ethanol, as the solvent, are shown in Fig. S3, see supplementary materials. This figure shows one strong, broad band at 319, 327, and 342 nm for 3-MeAPO, 3-Me-MeAPO, and 3-Me-PhAPO, respectively. The mentioned result for 3-MeAPO is near to the previously reported result, which had been reported as 316 nm by Ostercamp [59]. The corresponding experimentally UV band in APO had been reported at 299 and 300 nm in ethanol and methanol, respectively, by Ostercamp and Weinstein, respectively [59, 10]. The first 10 spin-allowed singlet–singlet excitations for the mentioned molecules were calculated by TD-DFT method at B3LYP/6-311++G** level for the same solvent, by using the PCM method. According to our theoretical results, the strongest theoretical band in 3-MeAPO, 3-Me-MeAPO, 3-Me-PhAPO, and APO are observed at 276, 280, 318 and 263 nm, respectively, which are attributed to the HOMO → LUMO with 99% major contributions of calculated transitions for APO and 3-MeAPO and about 80% for 3-Me-MeAPO and 3-Me-PhAPO. The theoretical and observed red shift for these bands in 3-MeAPO, 3-Me-MeAPO, and 3-Me-PhAPO, compared to the corresponding band in APO, is in excellent agreement with the average lengthening of the chelated ring components. The increase of the strength of IHB of 3-MeAPO, 3-Me-MeAPO, and 3-Me-PhAPO in comparison with the APO is in accord with the trend seen in (1), (see section 4).

The HOMO and LUMO represent the ability to donate and obtain an electron. Also, the energy gap between the HOMO and LUMO characterizes the chemical stability, reactivity and hardness of the molecule [60]. According to Fig. 3a-b, the HOMO-LUMO energy gaps of the studied molecules in 3-MeAPO, 3-Me-MeAPO, 3-Me-PhAPO, and APO are 3.71, 3.51, 3.17, and 3.98 eV, respectively. These energy gaps show that APO is more stable than the others.

4.5.3. Vibrational analysis

The IR and Raman spectra of 3-MeAPO and its deuterated isotopomer, D_2-3-MeAPO, in the CCl_4 solution and solid phase, are compared in Figs. S4-5, respectively. The effect of methyl substitution and dilution on the NH stretching of 3-MeAPO, is shown in Fig. 4. In this figure the

IR spectra of 3-MeAPO, D_2-3-MeAPO, and APO are compared in CCl_4 solution. For comparison also, the IR spectrum of 3-MeAPO in solid phase is shown in this figure. For confirmation of the assignment, when this is appropriate, the IR spectra of the title molecule are also compared with those of APO. The recorded Far IR spectra of 3-MeAPO and D_2-3-MeAPO in solid phase are shown in Fig. S6. The IR spectra of 3-MeAPO, D_2-3-MeAPO, and APO in the CCl_4 solution, in the 1700–900 cm^{-1} region, are compared in Fig. S7. The IR spectra of 3-MeAPO in the solid state and CCl_4 solution in the mentioned range are compared in Fig. S8. In addition, the IR spectra of 3-Me-MeAPO and 3-Me-PhAPO and their deuterated isotopomer, D-3-Me-MeAPO and D-3-Me-PhAPO, in the CCl_4 solution are shown in the Figs. S9-S10, supplementary materials. The computed frequencies of harmonic vibrational band and their approximate assignments, along with the experimental results of infrared and Raman frequencies for the stable aminoketone form of 3-MeAPO and its corresponding deuterated forms are presented in Tables 2 and 3, respectively. According to these tables, there are some differences between the calculated and experimental wavenumbers. These discrepancies are caused by several factors, such as anharmonicity, Fermi resonance, and solvent effects, which were not considered in our theoretical calculations.

4.5.3.1. Band assignment

The NH and CH stretching of amine, methyl, and methylene groups region

In this region, the NH/ND and C-H stretching vibrations are expected to be observed. In the amino compounds, the asymmetry and symmetrical NH stretching vibrations are expected to be observed in the 3520–3420 and 3420–3325 cm^{-1} regions, respectively [61, 62]. However, the existence of both intermolecular and intramolecular hydrogen bond systems perturbs this pattern [63]. For example, in CCl_4 solution, the ν_aNH band of APO and methyl 3-amino-2-butenoate (MAB) [11, 27] appear at 3375 and 3509 cm^{-1}, respectively. The ν_sNH band of the mentioned molecules appear at 3184 and 3335 cm^{-1}, respectively. While the theoretical and the other experimental results confirm that the strength of the intramolecular hydrogen bond (IHB) in APO is stronger than that in MAB [11, 27].

In the solid phase IR spectrum of 3-MeAPO, two strong bands were observed at 3280 and 3120 cm^{-1}, which upon deuteration shifts to 2476 and 2320 cm^{-1} (in the solid phase), respectively. The corresponding Raman bands of 3-MeAPO in the solid state appear at 3250 and 3095 cm^{-1}. According to our calculations, these bands are assigned to the NH asymmetrical and symmetrical stretching, respectively. However, in solutions the frequency of the former shifts considerably towards higher wavenumbers, appears at 3367 cm^{-1}, and its intensity decreases, while the position and intensity of the latter is almost constant, appears at about 3135 cm^{-1}, see Fig. 4 and Table 2. The positions of the corresponding bands in the solid phase of APO have been reported at about 3353 (3354) and 3179 (3179) cm^{-1}, the Raman values are in parenthesis [11], indicating that both intermolecular and intramolecular hydrogen bonds in 3-MeAPO are stronger than those in APO, which is in excellent agreement with the results of the DFT calculations and experimental ^{1}HNMR and UV spectra, see sections 4.4.1 and 4.4.2. The corresponding IR bands in the CCl_4 solution of D_2-3-MeAPO appear at 2595, 2562, 2520, and 2373 cm^{-1}. The first two bands are attributes to asymmetric ND_2 stretching in free and hydrogen bonded molecules. The last two bands are attributed to the overtones and symmetric ND_2 stretching modes, respectively. The corresponding IR bands in the solid phase of D_2-3-MeAPO are appeared at 2473, 2401, 2363, and 2320 cm^{-1}. The asymmetry and symmetry ND stretching bands of ND_2 in the Raman spectrum of D_2-3-MeAPO in the solid phase appear at 2476 and 2320 cm^{-1}, respectively.

The infrared spectrum of 3-MeAPO, in the CCl_4 solution, shows a weak band at about 3200 cm^{-1}, which upon dilution slightly shifts toward higher frequencies. We believe that this band is an overtone of IR band at 1624 cm^{-1}, which is in Fermi resonance with the 3135 cm^{-1} band.

The CH bond stretching of the CH_3 groups are expected to be appeared in the 2900–3000 cm^{-1} region [62, 64]. The IR spectrum of 3-MeAPO in the solid phase indicates 4 bands with relatively medium-intensity at 2985, 2965, 2923, and 2870 cm^{-1}, which are assigned to the CH stretching modes of the CH_3 groups. The corresponding Raman bands in 3-MeAPO observed at 3005, 2960, 2915, and 2880 cm^{-1}.

By considering the reported IR spectrum of 3-Me-PhAPO by Xiang Chen et al. [23], it seems that the NH stretching wavenumber, 3280 cm^{-1}, is not in agreement with our prediction. As explained in section 4.1, with increase of the IHBs, the N…O distance and NH str.

wavenumber decrease. Furthermore, the NH stretching wavenumbers should obey the trend (1). Moisture was removed by adding anhydrous Na_2SO_4 to the CCl_4 solution of the compounds. The IR spectrum of dried CCl_4 solution of 3-Me-PhAPO shows no band at about 3280 cm^{-1}, see Fig. S10 in supplementary material. As Figs. S9-10 show, the NH str. band cannot easily be identified. According to the N… O distance, we expect to observe the NH str. band frequencies at about 3000 cm^{-1}, which is overlapped with the CH str. bands. To estimate the NH str. wavenumber, we used the deuterated compounds (NH exchanged with deuterium). Since, the ND str. of 3-Me-MeAPO and 3-Me-PhAPO are 2270 and 2220 cm^{-1}, respectively, see Figs S9-10, so, the NH str. of the 3-Me-PhAPO is lower than that in 3-Me-MeAPO.

1700–1000 cm^{-1} region

In this region, as the most significant region of vibrational spectra, beside the CH_3 and NH_2 deformation and rocking modes, the C-CH_3, C-CN, C=O, C=C, and C-N stretching modes of the chelated ring are expected to be observed.

The IR spectrum of 3-MeAPO in the CCl_4 solution shows three strong bands at 1624, 1578, and 1491cm^{-1}. The corresponding IR bands in the solid phase appear at 1636 (as a shoulder), 1603, and 1498 cm^{-1} (see Fig. S8). In the Raman spectrum of 3-MeAPO in solid phase, the corresponding bands appear at 1571 and 1487 cm^{-1}. According to the theoretical results the band at 1624 cm^{-1} is assigned to ν_aOCCC coupled to $\delta_a CH_3(\beta)$. The corresponding band in the IR spectrum of APO in the CCl_4 solution occurs at 1630 cm^{-1}. We assign the other two IR strong bands at 1578 and 1491 cm^{-1} to the other normal modes, see Table 2. For APO, the corresponding bands appear at 1599 and 1536 cm^{-1}, respectively, see Fig. S7. The lower frequencies of these bands for 3-MeAPO, in the IR and Raman, in comparison with the corresponding values for APO confirm stronger hydrogen bond in 3-MeAPO compared with that in APO. The 1578 cm^{-1} band in the IR spectrum of 3-MeAPO, in the CCl_4 solution, is assigned to the NH_2 bending coupled with ν_sOCCC, ν_sCCCN, which upon deuteration, this band disappears, and new bands appear at about 1280 (1289) and 1206 (1193) cm^{-1}. The values of the Raman bands of D2-3-MeAPO are given in parenthesis.

By considering the theoretical calculations and comparing with the spectrum of APO [11], the medium to weak intensity IR bands at 1460-1350 cm^{-1} region, in the CCl_4 solution of 3-

MeAPO, which are not affected by deuteration (See Fig. S5), are assigned to δCH_3 which are coupled to some other motions. The corresponding Raman bands for CH_3 bending occur at 1463 and 1373 cm^{-1} in solid phase and at 1467 and 1377 cm^{-1} in the CCl_4 solution. The mentioned IR bands of APO, in the CCl_4 solution, appear at 1358-1425 cm^{-1} region (See Fig. S8).

The strong IR band in the CCl_4 solution of APO at 1282 cm^{-1} is assigned to the $\nu_s CCCN$, which is coupled to ρNH_2, $\rho CH_3(\beta)$. The mentioned IR band in 3-MeAPO, appears at 1259 cm^{-1}. The corresponding Raman bands in APO and 3-MeAPO appears at 1287 and 1278 cm^{-1}, respectively. A comparison between these bands, shows that this vibrational mode is shifted toward lower frequencies upon substitution of the CH_3 group in the α-position of APO and increases the IHB strength. This frequency shift is in excellent agreement with our calculated results and confirm our assignment. The calculated corresponding band in 3-MeAPO and APO are 1296 and 1317 cm^{-1}, respectively.

The weak and medium IR bands in the CCl_4 solution of 3-MeAPO at 1100-990 cm^{-1} and 970 cm^{-1} are assign to ρNH_2 and ρCH_3 vibrations coupled with the $\nu C\text{-}CH_3$ stretching mode, respectively. Upon deuteration, the intensity of these bands increases (See Fig. S4), which according the theoretical results, these bands are assigned to the ρCH_3, δND_2, and $\nu C\text{-}CH_3$ vibrational modes. The corresponding Raman bands appear at 1095, 1046, and 972 cm^{-1} (See Fig. S5). According to the theoretical results, the vibrational mode of ρND_2 in the IR spectra of D_2-3-MeAPO is observed at 843 cm^{-1}, as a medium-weak intensity band.

Below 1000 cm^{-1} region

In this region, we expect to observe the $C\text{-}CH_3$ stretching, N-H out of plane bending mode, and $C\text{-}CH_3$ in plane and out of plane bending modes and in plane and out of plane chelated ring deformations.

Theoretical calculation attributes the IR band at 875 cm^{-1} in the solid phase, to the $\nu C\text{-}CH_3$, which coupled with $\rho CH_3(\alpha)$ and in-plane chelated ring deformation, Δ. The mentioned normal mode in the IR spectrum of D_2-3-MeAPO appears at 877 cm^{-1}. The above Raman bands are at 875 and 878 cm^{-1}. In the solid state a relatively IR broad band, which upon deuteration disappears, is observed at 798 cm^{-1}, we assigned this band to the torsion of NH_2. The mentioned IR band in MAB has been observed at 692 cm^{-1} [27].

According to our calculations, in the solid-state IR spectrum of 3-MeAPO, the weak intensity band at 798 cm^{-1} is assigned to the out-of-plane NH bending which disappears upon deuteration. The corresponding vibration in APO and MAB is strongly coupled with the out-of-plane CH_α bending. In the solid-state IR spectrum of APO, the coupled vibrations appear at 818 and 755 cm^{-1}, its averaged is 786 cm^{-1}, while in solid MAB it is reported to be occurred at 772 cm^{-1} [11, 27]. These values confirm that the intramolecular hydrogen bond in 3-MeAPO is stronger than that in APO and MAB.

The out of plane bending of chelated ring, Γ, appears in the solid phase IR spectrum of 3-MeAPO at 645 cm^{-1}, as strong intensity band. The corresponding band in APO appeared at 630 cm^{-1} [11]. This result is also in agreement with the stronger of hydrogen bond in 3-MeAPO compared to that in APO.

The infrared spectrum of 3-MeAPO in the CCl_4 solution shows a shoulder band at 430 cm^{-1}, which in the solid phase this band splits to two medium bands and observed at 450 and 432 cm^{-1}. According to the theoretical calculating, this band is assigned to the in-plane deformation of the chelated ring (Δ). The corresponding bands in the Raman spectra of 3-MeAPO in the solid and solution phase are observed at 451 and 445 cm^{-1}, respectively. The corresponding band in the IR and Raman spectra of MAB reported at lower frequency, 399 and 408 cm^{-1}, respectively [27]. This shift also shows that the IHB strength in 3-MeAPO is more than that in MAB.

By considering the theoretical calculation and comparing with the vibrational spectra of APO and MAB, the IR band at 380 cm^{-1} in the CCl_4 solution of 3-MeAPO is assigned to the N…O stretching, coupled with $\delta C\text{-}CH_3$. The corresponding band in APO and MAB appeared at 360 and 344 cm^{-1}, respectively, [27], which also supports the stronger IHB in 3-MeAPO than that in APO and MAB. These frequency shifts are in excellent agreement with the UV, NMR, DFT, and the other IR bands related to IHB strength. The Raman band of this normal mode in the solid phase of APO and 3-MeAPO appears at 360 and 404 cm^{-1}, respectively. Upon deuteration, the mentioned IR and Raman bands are appeared slightly lower than the observed values for 3-MeAPO, which are consistent with the theoretical results.

According to the theoretical results, the IR band at 289 cm^{-1} in the solid phase of 3-MeAPO is assigned to the out-of-plane of chelated ring deformation coupled with $\gamma C\text{-}CH_3$ (β), for which the corresponding Raman band appears at 292 cm^{-1}. The IR and Raman bands of this normal mode in D_2-3-MeAPO are observed at 289 and 284 cm^{-1}, respectively.

5. Conclusion

According to our theoretical and experimental results, among 3 possible tautomers of 3-MeAPO, the aminoketone tautomer is the most stable form. In addition, from the theoretical point of view, by considering the conformations of the CH_3 groups in 3-MeAPO, with respect to the plane of the molecule, 8 aminoketone conformers can be drawn for that. Among them, only one conformer of aminoketone tautomer is stable at the B3LYP/6-311++G** level calculations. The structures of the other conformers turn under full optimization to the stable form, AK1.

The crystal structure of 3-MeAPO was determined by single crystal X-ray diffraction. There is an excellent agreement between the X-ray result and the calculated molecular structure. In addition, the molecular structure, vibrational, UV, and NMR spectra, of 3-MeAPO and its deuterated analogue, D_2-3-MeAPO, were predicted using DFT calculations at the mentioned level. A complete vibrational assignment of the 3-MeAPO compound is presented. The infrared spectra also show that in the solid state, 3-MeAPO is not only engaged in an intramolecular hydrogen bond, but also forms an intermolecular hydrogen bond. In addition, the intermolecular hydrogen bond will disappear in dilute CCl_4 solutions. All theoretical and experimental results include vibrational, NMR, and UV spectra show that the following trend in IHB strength is obtained:

3-Me-PhAPO > 3-Me-MeAPO > 3-MeAPO > APO

This result could be attributed to the steric effect of CH_3 group in the α-position with the hydrogen atoms of methyl groups in the β position, which pushes the methyl groups toward oxygen and nitrogen atoms. In addition, the NBO results show, the steric effect of methyl and phenyl substitutions on the nitrogen atom also causes to decrease the N…O distance and increase the IHB strength.

Acknowledgement

This work was supported by the Ferdowsi University of Mashhad, Grant No. 42561.

The authors wish to thank Kristina Eriksen (Ph.D, Copenhagen University) for her valuable help in the analysis of the X-ray data and Eva Marie Karlsen (Roskilde University) for scanning of IR and UV spectra of 3-Me-MeAPO and 3-Me-PhAPO molecules.

Appendix A. Supplementary material

Supplementary data associated with this article can be found, in the online version, at http://dx.doi.org/??.????/ Journal of molecular structure,??.??.??.

References:

[1] A. Jamshidvand, M. Sahihi, V. Mirkhani, M. Moghadam, I. Mohammadpoor-Baltork, S. Tangestaninejad, H. Amiri Rudbari, H. Kargar, R. Keshavarzi, S. Gharaghani, Studies on DNA binding properties of new Schiff base ligands using spectroscopic, electrochemical and computational methods: Influence of substitutions on DNA-binding, J. Mol. Liquids, 253 (2018) 61–71.

[2] I. O. Idafiogho, K. V. V. Ananthalakshmi, S. B. Combian, Anticonvulsant evaluation and mechanism of action of benzyl amino enaminones, Bioorg. Med. Chem., 14 (2006) 5266–5272.

[3] A. Vanicat, C. André-Barrès, E. Delfourne, New reaction of formation of the fused tricyclic bispyrroloquinone ring system, Tetrahedron Letters, 58 (2017) 342–345.

[4] G. Palmieri, C. Cimarelli, Chemo- and stereoselective reduction of enaminones for the preparation of biologically active compounds, ARKIVOC, (2006) 104–126.

[5] P. E. Hansen, R. Kawecki, A. Krowczynski, L. Kozerski, Deuterium Isotope Effects on ^{13}C and ^{15}N Nuclear Shielding in Intramoleculary Hydrogen-bonded Compounds. II. Investigation of Enamine Derivatives, Acta Chem. Scand., 44 (1990) 826-832.

[6] S. I. Vdovenko, I. I. Gerus, Y. I. Zhuk, V. P. Kukhar, M. Pagacz-Kostrzewa, M. Wierzejewska, C. G. Daniliuc, The conformational analysis of push-pull enaminones using FTIR and NMR spectroscopy, and quantum chemical calculations. VI. β-N-Methyl-aminovinyl trifluoromethyl ketone and α-methyl-β-N-methylaminovinyl trifluoromethyl ketone, J. Mol. Structure, 1128 (2017) 741-753.

[7] D. K. Zheglova, D. G. Genov, S. Bolvig, P. E. Hansen, Deuterium Isotope Effects on ^{13}C Chemical Shifts of Enaminones, Acta Chem.Scand., 51 (1997) 1016-1023.

[8] S. F. Tayyari, M. Fazli, F. Milani-nejad, Molecular conformation and intramolecular hydrogen bonding in 4-amino-3-penten-2-one, J. Mol. Struct. (Theochem.), 541 (2001) 11-15.

[9] H. Eshghi, S. M. Seyedi, E. Safaei, M. Vakili, A. Farhadipour, M. Bayat-Mokhtari, Silica supported Fe $(HSO_4)_3$ as an efficient, heterogeneous and recyclable catalyst for synthesis of β-enaminones and β-enamino esters, J. Mol. Cat. A: Chemical, 363– 364 (2012) 430– 436.

[10] J. Weinstein, G. M. Wyman, A study of β-amino-α, β-unsaturated ketones, J. Org. Chem., 23 (1958) 1618–1622.

[11] S. F. Tayyari, H. Raissi, F. Tayyari, Vibrational assignment of 4-amino-3-penten-2-one, Spectrochim. Acta Part A, 58 (2002) 1681–1695.

[12] V. Bertolasi, L. Pretto, V. Ferretti, P. Gilli, G. Gilli, Interplay between steric and electronic factors in determining the strength of intramolecular N—H...O resonance-assisted hydrogen bonds in β-enaminones Acta Crystallogr., B 62 (2006) 1112–1120.

[13] G. O. Dudeck, G. P. Volpp, Nuclear Magnetic Resonance Studies of Keto-Enol Equilibria. V. Isomerization in Aliphatic Schiff Bases, J. Am. Chem. Soc., 85 (1963) 2697–2702.

[14] P. Gilli, V. Bertolasi, V. Ferretti, G. Gilli, Evidence for Intramolecular N−H···O Resonance-Assisted Hydrogen Bonding in β-Enaminones and Related Heterodienes. A Combined Crystal-Structural, IR and NMR Spectroscopic, and Quantum-Mechanical Investigation, J. Am. Chem. Soc., 122 (2000) 10405–10417.

[15] P. E. Hansen, J. Sitkowski, L. Stefaniak, Z. Rozwadowski, T. Dziembowska; One Bond Deuterium Isotope Effects on ^{15}N Chemical Shifts, $^{1}\Delta^{15}N(D)$, in Schiff Bases, Berichte Bunsengesel Chem. Phys., 102 (1998) 410-413.

[16] A. Filarowski, A. Koll, M. Rospenk, I. Krol-Starzomska, P. E. Hansen, Tautomerism of sterically hindered Schiff bases. Deuterium Isotope Effects on ^{13}C Chemical Shifts, J. Phys. Chem. A., 109 (2005) 4464-73.

[17] G. Desiraju, T. Steiner, The weak hydrogen bond in structural chemistry and biology, Oxford University Press, Oxford, 1999.

[18] G. A. Jeffrey, W. Saenger, Hydrogen bonding in biological structures, Springer, New York, 1991.

[19] S. Deechongkit, P. E. Dawson, J. W. Kelly, Toward assessing the position-dependent contributions of backbone hydrogen bonding to beta-sheet folding thermodynamics employing amide-to-ester perturbations, J Am Chem Soc., 126 (51) (2004) 16762–16771.

[20] J. C. Noveron, M. S. Lah, R. E. Del Sesto, A. M. Arif, J. S. Miller, P. J. Stang, Engineering the structure and magnetic properties of crystalline solids via the metal-directed self-assembly of a versatile molecular building unit, J. Am. Chem. Soc., 126 (2004) 6613–6625.

[21] S. Gogoi, R. Bhuyan, N. C. Barua, Iodine-Catalyzed Conversion of beta-Dicarbonyl Compounds into beta-Enaminones Within a Minute Under Silvent-Free Conditions, Synthetic Communications, 35 (2005) 2811-2818.

[22] M. E. F. Braibante, H. S. Braibante, L. Missio, A. Andricopulo, Synthesis and Reactivity of beta -Amino alpha,beta-Unsaturated Ketones and Esters Using K-10 Montmorillonite, Synthesis, 09 (1994) 898-900.

[23] X. Chen, J. She, Z. Shang, J. Wu, H. Wu, P. Zhang, Synthesis of Pyrazoles, Diazepines, Enaminones, and Enamino Esters Using 12-Tungstophosphoric Acid as a Reusable Catalyst in Water, SYNTHESIS, 21 (2008) 3478-3486.

[24] H. F. Holtzclaw, J. James, P. Collman, R. M. Alire, Syntheses and Infrared Spectra of alpha,beta-Unsaturated-beta-ketoamines and thier Copper Chelates, J. Am. Chem. Soc., 80 (1958) 1100-1103.

[25] G. Buemi, F. Zuccarello, P. Venuvanalingam, M. Ramalingam, Ab initio study of tautomerism and hydrogen bonding of beta-carbonylamine in the gas phase and in water solution, Theor. Chem. Acc., 104 (2000) 226-234.

[26] R. W. F. Bader, Atoms in Molecules. A Quantum Theory, Oxford University Press, New York, 1990.

[27] A. R. Berenji, S. F. Tayyari, M. Rahimizadeh, H. Eshghi, M. Vakili, A. Shiri, Structure and vibrational analysis of methyl 3-amino-2-butenoate, Spectrochimica Acta Part A: Molecular and Biomolecular Spectroscopy, 102 (2013) 350–357.

[28] M. J. Lacey, Convenient syntheses of 4-Aminopent-3-en-2-one and its copper and nickel complexes, Aust. J. of Chem., 23(4) (1970) 841-842.

[29] D. L. Ostercamp, Vinylogous Imides. I. Nuclear Magnetic Resonance Spectra, J. Org. Chem., 30 (4) (1965) 1169-1174.

[30] F. Strübe, S. Rath, J. Mattay, Functionalized Fulgides and Fluorophore-Photoswitch Conjugates, European Journal of Organic Chemistry, 24 (2011) 4645–4653.

[31] T. Mikysek, H. Kvapilova, H. Dousova, F. Josefik, P. Simunek, Z. Ruzickova, J. Ludvik, Synthesis, electrochemical, structural and theoretical study of new drivatives of OBN and OBO heterocycles, Inorganica Chimica Acta, 455 (2017) 465-472.

[32] M. Ghaffari, M.Sc. Thesis, Ferdowsi University of Mashhad, Mashhad, 2010.

[33] O. V. Dolomanov, L. J. Bourhis, R. J. Gildea, J. A. K. Howard and H. Puschmann, OLEX2: a complete structure solution, refinement and analysis program, J. Appl. Cryst., 42 (2009) 339-341.

[34] L. J. Bourhis, O. V. Dolomanov, R. J. Gildea, J. A. K. Howard and H. Puschmann, The anatomy of a comprehensive constrained, restrained refinement program for the modern computing environment - Olex2 dissected, Acta Cryst., A71 (2015) 59-75.

[35] G. M. Sheldrick, Crystal structure refinement with SHELXL, Acta Cryst. C71 (2015) 3-8.

[36] M. J. Frisch, G. W. Trucks, H. B. Schlegel, G. E. Scuseria, M. A. Robb, J. R. Cheeseman, G. Scalmani, V. Barone, B. Mennucci, G. A. Petersson, H. Nakatsuji, M. Caricato, X. Li, H.P. Hratchian, A. F. Izmaylov, J. Bloino, G. Zheng, J. L. Sonnenberg, M. Hada, M. Ehara, K. Toyota, R. Fukuda, J. Hasegawa, M. Ishida, T. Nakajima, Y. Honda, O. Kitao, H. Nakai, T. Vreven, J. A. Montgomery, Jr., J. E. Peralta, F. Ogliaro, M. Bearpark, J. J. Heyd, E. Brothers, K. N. Kudin, V. N. Staroverov, R. Kobayashi, J. Normand, K. Raghavachari, A. Rendell, J. C. Burant, S. S. Iyengar, J. Tomasi, M. Cossi, N. Rega, J. M. Millam, M. Klene, J. E. Knox, J. B. Cross, V. Bakken, C. Adamo, J. Jaramillo, R. Gomperts, R. E. Stratmann, O. Yazyev, A. J. Austin, R. Cammi, C. Pomelli, J. W. Ochterski, R. L. Martin, K. Morokuma, V. G. Zakrzewski, G. A. Voth, P. Salvador, J. J. Dannenberg, S. Dapprich, A. D. Daniels, O. Farkas, J. B. Foresman, J. V. Ortiz, J. Cioslowski, D. J. Fox, Gaussian 09, Revision A.02, Gaussian Inc., Wallingford CT, 2009.

[37] F. W. Biegler-King, J. Schnbohm, D. Bayles, Software news and updates-AIM2000-A program to analyze and visualize atoms in molecules, J. Comp. Chem. 22 (2001) 545–559.

[38] NBO 5.0. E. D. Glendening, J. K. Badenhoop, A. E. Reed, J. E. Carpenter, J. A. Bohmann, C. M. Morales, F. Weinhold, Theoretical Chemistry Institute, University of Wisconsin, Madison, WI, 2001. <http://www.chem.wisc.edu/nbo5>.

[39] A. D. Becke, Becke's three parameter hybrid method using the LYP correlation functional, J. Chem. Phys., 98 (1993) 5648–5652.

[40] C. Lee, W. Yang, R. G. Parr, Development of the Colle-Salvetti correlation-energy formula into a functional of the electron density, Phys. Rev., 37B (1988) 785–789.

[41] GaussView 4.1.2, Gaussian Inc., Pittsburgh, PA, 2006.

[42] A. E. Reed, L. A. Curtiss, F. Weinhold, Intermolecular interactions from a natural bond orbital, donor-acceptor viewpoint., Chem. Rev., 88 (1988) 899-926.

[43] V. F. Weisskopf, Of Atoms, Mountains, and Stars: A Study in Qualitative Physics, Science, 187 (1975) 605-612.

[44] R. McWeeny, Perturbation Theory for the Fock-Dirac Density Matrix, Phys. Rev., 126 (1962) 1028–1034.

[45] J. L. Dodds, R. McWeeny, A. J. Sadlej, Self-consistent perturbation theory, Mol. Phys., 41 (1980) 1419–1425.

[46] J. Tomasi, M. Persico, Molecular interactions in solution: an overview of methods based on continuous distributions of the solvent, Chem. Rev., 94 (1994) 2027-2094.

[47] T. N. Hill, A. Roodt, Solid-state and Computational Study of “Venus fly-trap” Geometric Parameters for 1,5-Cyclooctadiene in Pd^{II} and Pt^{II} β-Enaminonato Complexes, Journal of Inorganic and General Chemistry, Z. Anorg. Allg. Chem. 644 (2018) 763–774.

[48] I. V. Svistunova, A. V. Gerasimenko, V. V. Korochentsev, N. P. Shapkin, V. I. Vovna, A study of the crystal structure of chloro-and bromo-substituted acetylacetonates of boron difluoride, J. Struct. Chem., 53 (2012) 1105-1110.

[49] S. Seyedkatouli, M. Vakili, S. F. Tayyari, R. Afzali, Molecular structure, spectroscopic studies, and copper-oxygen bond strength, of α-methyl and α-ethyl derivatives of copper (II) acetylacetonato; Experimental and theoretical approach, J. Mol. Structure, 1160 (2018) 107-116.

[50] C. L. Perrin, Are Short, Low-Barrier Hydrogen Bonds Unusually Strong?, Acc. Chem. Res., 43 (2010) 1550-1557.

[51] N. V. Belova, N. H. Trang, H. Oberhammer, G. V. Girichev, Tautomeric and conformational properties of dipivaloylmethane, J. Mol. Structure, 1132 (2017) 63-69.

[52] M. Cuma, S. Scheiner, T. Kar, Competition between rotamerization and proton transfer in o-hydroxybenzaldehyde, J. Am. Chem. Soc., 120 (1998) 10497-10503.

[53] M. Jablonski, A. Kaczmarek, A. J. Sadlej, Estimates of Energy of Intramolecular Hydrogen Bonds, J. Phys. Chem A., 110 (2006) 10890-10898.

[54] E. Espinosa, E. Molins, C. Lecomte, Hydrogen bond strengths revealed by topological analyses of experimentally observed electron densities, Chem. Phys. Lett., 285 (1998) 170–173.
[55] A. V. Afonin, I. V. Sterkhova, A. V. Vashchenko, M. V. Sigalov, Estimating the energy of intramolecular bifurcated (three-centered) hydrogen bond by X-ray, IR and 1H NMR spectroscopy, and QTAIM calculations, J. Mol. Structure, 1163 (2018) 185-196.
[56] I. Rozas, I. Alkorta, J. Elguero, Behavior of Ylides Containing N, O, and C Atoms as Hydrogen Bond Acceptors, J. Am. Chem. Soc., 122 (2000) 11154–11161.
[57] P. E. Hansen, Isotope Effects on Chemical Shifts of Hydrogen Bonded Systems, J. Label. Comp. Radiopharm., 50 (2007) 967-981.
[58] P. E. Hansen, A. Kolonicny, A. Lycka, Deuterium Isotope Effects on ^{13}C Nuclear Shielding of Amino and Acetamido Compounds. Tautomerism and Intramolecular Hydrogen-bonding, Magn. Reson. Chem., 30 (1992) 786-96.
[59] D. L. Ostercamp, Vinylogous Imides. II. Ultraviolet Spectra and the Application of Woodward's Rules, J. Org. Chem., 35 (5) (1970) 1632–1641.
[60] L. David, C. Craciun, O. Cozar, V. Chis, C. Agut, D. Rusu, M. Rusu, Spectroscopic studies of some oxygen-bonded copper (II) β-diketonate complexes, J. Mol. Structure, 563-564 (2001) 573-578.
[61] A. R. Katritzky, R. A. Jones, Infrared absorption of substituents in heteroaromatic systems. Part III. Amino-, methylamino-, and dimethylamino-compounds, J. Chem. Soc., (1959) 3674–3679.
[62] M. Madhab Borah, Th. Gomti Devi, Vibrational studies of Thyroxine hormone: Comparative study with quantum Chemical calculations, J. Mol. Structure, 1148 (2017) 293-313.
[63] J. N. Gardner, A. R. Katritzky, N-oxides and related compounds. Part V. The tautomerism of 2- and 4-amino- and -hydroxy pyridine 1-oxide, J. Chem. Soc., (1957) 4375–4385.
[64] N. B. Colthup, L.H. Daly, S.E. Wiberley, Introduction to Infrared and Raman spectroscopy, Academic Press, London, 1975.

Caption for Figures

Fig 1: Tautomery in β-ketoenamines.

Fig 2: a) ORTEP structure of 3-MeAPO. b, c, d) the optimized structures at B3LYP/6-311++G** level, of 3-MeAPO, 3-Me-PhAPO, and 3-Me-MeAPO, respectively.

Fig 3: The calculated HOMO-LUMO energy gaps: a) for the 3-MeAPO and APO. b) for the 3-Me-MeAPO and 3-Me-PhAPO.

Fig. 4: The recorded infrared spectra of APO (…), 3-MeAPO (———), and D_2-3-MeAPO (—…—…) in CCl_4, 3-MeAPO (– – – –) in solid phase (in the 3500–2700 cm-1 range).

Supplementary material

Fig. S1: The atom numbering and conformations for aminoketone form of 3-MeAPO, only AK1 is stable by calculations at B3LYP/6-311++G** level.

Fig. S2: The recorded NMR spectra of 3-MeAPO, 3-Me-PhAPO, and 3-Me-MeAPO in $CDCl_3$: a, c, e) ^{1}HNMR and b, d, f) ^{13}CNMR.

Fig. S3: The recorded experimental UV-Vis spectra of 3-MeAPO, 3-Me-MeAPO, and 3-Me-PhAPO in ethanol as solvent.

Fig. S4: The recorded infrared spectra of 3-MeAPO (———) and its deuterated analogue (……) in CCl_4 (in the 1700–900 cm^{-1} range).

Fig. S5: The recorded Raman spectra of 3-MeAPO (———) and D_2-3-MeAPO (……) in solid phase (in the 3300–200 cm^{-1} range).

Fig. S6: The recorded Far IR spectra of 3-MeAPO (———) and D_2-3-MeAPO (……) in solid phase (in the 620–250 cm^{-1} range).

Fig. S7: The recorded infrared spectra of 3-MeAPO (———), APO (……), and D_2-3-MeAPO (– – – –) in CCl_4 (in the 1700–900 cm^{-1} range).

Fig. S8: The recorded infrared spectra of the 3-MeAPO in the solid phase and CCl_4 solution (in the 1800–800 cm^{-1} range).

Fig. S9: The recorded infrared spectra of 3-Me-MeAPO (———) and D-3-Me-MeAPO (……) in CCl_4 (in the 3200–800 cm^{-1} range).

Fig. S10: The recorded infrared spectra of 3-Me-PhAPO (———) and D-3-Me-PhAPO (……) in CCl_4 (in the 3200–900 cm^{-1} range).

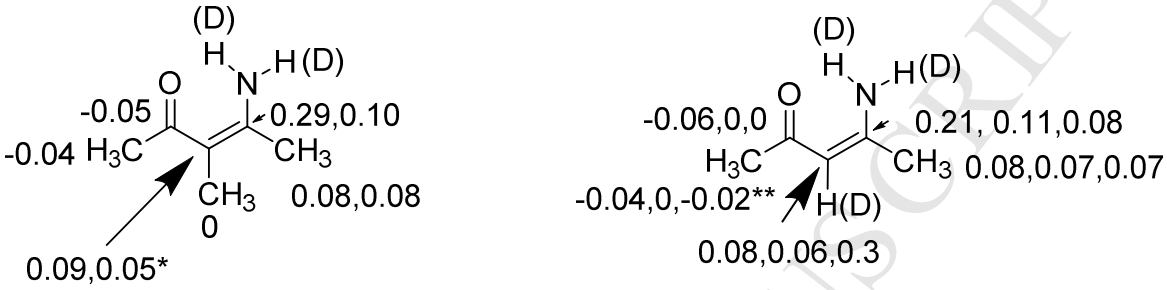

Scheme 1. Deuterium isotope effects on ^{13}C chemical shifts of 3-MeAPO and APO. For 3-MeAPO the order is deuterium at the hydrogen bonded position, deuterium at the non-hydrogen bonded position. For APO the last number is for deuteration at C-3.

* The central line is broad, so isotope effects cannot be measured accurately.

****** Assignment tentative.

Table 1

Some selected theoretical parameters of 3-MeAPO, 3-Me-MeAPO, 3-Me-PhAPO, and APO calculated at B3LYP/6-311++G** level of theory (bond lengths and bond angles are in Å and °, respectively) and the mentioned experimental parameters of 3-MeAPO.

	3-MeAPO		3-Me-MeAPO	3-Me-PhAPO	APO	
	Theoretical	X-ray	Theoretical	Theoretical	Theoretical	[27] [a]
Bond length						
C2-C3	1.453	1.4248(15)	1.448	1.451	1.443	1.442
C4-C3	1.387	1.3915(15)	1.396	1.393	1.377	1.378
C4-N	1.350	1.3371(16)	1.349	1.359	1.348	1.347
C2-O	1.244	1.2625(14)	1.249	1.248	1.242	1.242
C2-C1	1.521	1.5123(15)	1.524	1.521	1.518	….
C4-C5	1.511	1.5046(15)	1.508	1.509	1.505	1.505
N-H9	1.020	0.9231	1.025	1.032	1.019	1.019
N-H10	1.005	0.8865	…..	…..	1.006	1.006
O...H9	1.802	1.8738	1.732	1.702	1.890	1.885
N...O6	2.597	2.6187(16)	2.584	2.581	2.669	2.666
Bond angles						
C2C3C4	120.0	120.27(10)	120.0	120.7	123.1	123.0
C3C4C5	122.6	121.80(10)	121.9	120.6	121.6	121.6
C3C2C1	118.4	118.13(10)	119.8	119.4	117.0	…..
OC2C3	123.7	124.26(9)	123.3	123.3	123.1	123.1
C4NH9	117.1	115.44	113.2	111.8	117.3	…..
C4NH10	120.7	120.00	…..	…..	121.4	…..
C5C4N	115.0	115.16(9)	116.2	118.5	116.3	116.3
C1C2O	118.0	117.61(9)	116.9	117.3	119.5	…..
OH9N	131.9	135.76	137.6	140.3	130.8	130.9
DA (°) [b]						
C5C4NH9	180.0	178.0	-179.1	172.3	-179.9	179.8
C3C4NH9	0.0	2.2	1.2	-4.4	0.1	-0.2
C3C4NH10	180.0	173.5	…..	…..	179.8	-179.6
OC2C3C4	0.0	3.9(17)	2.8	-1.2	-0.5	0.2
NC4C3C2	0.0	-2.9(16)	-3.0	2.5	0.3	0.0
AIM results [c]						
ρ_{BCP}	0.039	….	0.046	0.049	0.031	….
∇^2_{BCP}	-0.0345	….	-0.0376	-0.0383	-0.0277	….
E_{HB}	10.85	….	13.63	14.91	7.67	….

[a] Data from [27].

[b] DA is dihedral angle.

[c] Charge density (ρ) in e.au^{-3}, Laplacian of charge density ($\nabla^2\rho$) in (e.au^{-5}) at the bond critical point (BCP) of the O…H bond. E_{HB} is the IHB energy in kcal/mol, according to Espinosa et al. suggestion [54].

Table. 2

Fundamental band assignment of 3-MeAPO (frequencies in cm^{-1}). [a]

Theoretical			Experimental				Assignment
Freq.	I_{IR}	A_R	IR (solid)	IR(CCl_4)	R(solid)	R(CCl_4)	
				3500(25)			νNH10(free)
3693	77	117	3280(78)	3367(11)	3250(14)	3240(10)	ν_aNH_2
				3200(4)			2*1624
3397	101	79	3120(71)	3135(8)	3095(16)	3080(12)	ν_sNH_2
3137	11	77	2985(46)	2997(9)	3005(3)	2995(2)	$\nu_aC1H_3(\beta)$
3120	20	60	2965(sh)	2962(11)	2960(23)	2948(22)	$\nu_aCH_3(\alpha)$, $\nu_aC5H_3(\beta)$
3105	25	50	2923(40)	2925(13)	2915(33)	2911(40)	$\nu_aCH_3(\alpha)$, $\nu_aC5H_3(\beta)$
3100	7	60	2923	2925	2915	2911	$\nu_aC5H_3(\beta)$
3081	15	65	2870(32)	2875(11)	2880(90)	2875(100)	$\nu_aC1H_3(\beta)$
3043	27	83	2870	2875	2880	2875	$\nu_aCH_3(\alpha)$
3038	12	217	2870	2875	2880	2875	$\nu_sC5H_3(\beta)$
3028	16	216	2870	2875	2880	2875	$\nu_sC1H_3(\beta)$
3010	47	149	2870	2875	2880	2875	$\nu_sCH_3(\alpha)$
1669	234	5	1636(sh)	1624(99)			ν_aOCCC, $\delta_aCH_3(\beta)$
1622	326	20	1603(93)	1578(86)	1571(24)	1560(16)	δNH_2, ν_sOCCC, ν_sCCCN
1529	201	29	1498(85)	1491(94)	1487(78)	1478(41)	ν_sOCCC, ν_aCCCN, δNH_2, $\delta_aCH_3(\alpha)$
1509	52	14	1498	1491	1487	1478	δNH_2, $\delta_aCH_3(\alpha,\beta)$, ν_sOCCC
1504	4	8	1498	1491	1487	1478	$\delta_aCH_3(\alpha,\beta)$
1488	45	25	1462(66)	1460(sh)	1463(sh)	1456(sh)	$\delta_aCH_3(\alpha,\beta)$, $\nu_aCC\alpha C$
1480	24	0	1441(sh)	1438(sh)			$\delta_aCH_3(\beta)$
1474	1	16	1441	1438			$\delta_aCH_3(\alpha,\beta)$
1464	44	6	1426(sh)	1421(28)			$\delta_aC1H_3(\beta)$
1428	7	14	1399(34)	1393(17)			$\delta_sCH_3(\alpha)$
1417	3	0	1399	1393			$\delta_sCH_3(\alpha)$, $\delta_sC5H_3(\beta)$, δNH_2, ν_aCN, νCO
1399	9	9	1371(47)	1368(27)	1373(67)	1371(35)	$\delta_sCH_3(\beta,\alpha)$, δNH_2, ν_aNCCC
1384	35	3	1350(41)	1354(30)		1346(sh)	$\delta_sC1H_3(\beta)$, δNH_2, νNC
1296	170	4	1270(48)	1259(71)	1278(12)	1272(12)	ν_sCCCN, ρNH_2, $\rho CH_3(\beta,\alpha)$, νC-$CH_3(\alpha)$
1243	19	9	1220(56)	1227(20)	1224(42)	1218(24)	νC-$CH_3(\alpha)$, ρNH_2, $\rho CH_3(\beta)$
				1145(6)			combination?
1109	6	5	1091(17)	1104(5)	1095(28)	1086(12)	ρNH_2, $\rho CH_3(\alpha)$, νC-$CH_3(\beta)$
1062	1	0	1046(8)	1044(4)	1046(10)	1033(7)	$\rho CH_3(\alpha,\beta)$
1049	0	0	1046	1044			$\rho CH_3(\alpha,\beta)$
1039	6	3	1046	1040(5)		1040(sh)	ρNH_2, $\rho CH_3(\beta)$, νC-$CH_3(\alpha)$
1026	2	0	1012(sh)	1009(10)			$\rho CH_3(\alpha,\beta)$
1011	20	1	1001(31)	996(12)			$\rho CH_3(\alpha,\beta)$, ρNH_2, νC-CH_3
982	76	5	970(64)	970(48)	972(11)	966(6)	$\rho CH_3(\alpha,\beta)$
881	6	1	875(19)	872(7)	875(5)	869(4)	νC-CH_3, $\rho CH_3(\alpha)$, Δ
788	33	0	798(6)				γNH_2
694	7	19	690(sh)	687(45)	695(81)	691(54)	δC-$CH_3(\alpha,\beta)$, νC-$CH_3(\alpha)$
641	3	0	645(100) *	626(22) *			Γ, γNH9
603	7	4	597(97)	600(29)	601(10)	595(5)	$\delta CC_\alpha C$, νN…O, δCO, δNH9
547	8	1	543(80)	541(27)	545(14)	539(10)	Γ

501	1	0	512(73)		513(7)		δCH_3-CN, δCH_3-CO
436	5	5	432(92), 450(89)	430(sh)	451(28)	445(19)	Δ
394	3	7	405(93)	380(100)	404(65)	398(31)	νN…O, δC-CH_3(β)
344	1	0					δC-CH_3(α,β), Δ
284	1	1	289(80)		292(38)	290(29)	Γ, γC-CH_3(α)
270	5	0					νN…O, δC-CH_3(β)
263	135	0					γNH_2
160	1	1					τCH_3(α,β)
132	4	0					τCH_3(β)
129	1	1					τCH_3(α,β), Γ
79	12	0					γC-CH_3(α,β), γNH10
23	2	0					τCH_3(α,β)

[a] Freq., vibrational wavenumber (calculated at the B3LYP/6-311++G** level); I_{IR}, IR intensities in kM/mol; A_R., Raman scattering activities in A**4/AMU; experimental relative intensities are given in parenthesis; sh, shoulder; n.m., not measured; ν, stretching; δ, in-plane bending; γ, out-of-plane bending; ρ, rocking; Δ, in-plane chelated ring deformation; Γ, out-of-plane chelated ring deformation; τ, torsion; *, below 700 cm^{-1}obtained with different instrument.

Table. 3

Fundamental band assignment of D_2-3-MeAPO (frequencies in cm^{-1}). [a]

Theoretical			Experimental			Assignment
Freq.	I_{IR}	A_R	IR (solid)	IR(CCl_4)[b]	R(solid)	
3138	12	76	2985(20)		2981(2)	$\nu_aC1H_3(\beta)$
3119	19	63	2963(19)		2952(2)	$\nu_aCH_3(\alpha)$, $\nu_aC5H_3(\beta)$
3106	27	49	2923(27)		2917(5)	$\nu_aC5H_3(\beta)$,$\nu_aCH_3(\alpha)$
3100	7	60	2923		2917	$\nu_aC5H_3(\beta)$
3082	15	65	2875(16)		2880(80)	$\nu_aC1H_3(\beta)$
3043	27	84	2875		2880	$\nu_aCH_3(\alpha)$
3039	12	221	2875		2880	$\nu_sC5H_3(\beta)$
3029	16	213	2875		2880	$\nu_sC1H_3(\beta)$
3010	46	149	2875		2880	$\nu_sCH_3(\alpha)$
			2855(14)			2*1437
				2800(14)		2*1418
				2595(14)		νND_2(free)
2725	64	48	2473(48)	2562(11)	2476(8)	ν_aND_2
				2520(sh)		overton
			2401(31)			overton
			2363(36)			overton
2468	63	43	2320(53)	2373(18)	2320(13)	ν_sND_2
1666	244	5	1603(100)	1622(100)		$\nu_aOCC_\alpha C$
1541	379	57	1496(75)	1497(87)	1500(sh)	$\nu_sOCC_\alpha C$, δND_2, $\delta_aCH_3(\alpha,\beta)$
1518	4	4	1476(sh)	1476(sh)	1473(sh)	$\delta_aCH_3(\alpha)$, $\delta_aC5H_3(\beta)$, νCN
1504	5	8	1457(sh)	1460(47)	1473	$\delta_aCH_3(\alpha,\beta)$
1485	80	25	1439(87)	1438(40)	1434(67)	$\delta_aCH_3(\alpha)$, $\delta_aC5H_3(\beta)$, $\nu_aCC_\alpha C$, δND_2
1480	21	0	1439	1438(sh)		$\delta_aCH_3(\beta)$
1473	2	16	1439	1438	1434	$\delta_aCH_3(\alpha,\beta)$
1464	62	7	1439	1421(46)	1434	$\delta_aC5H_3(\beta)$
1444	44	4	1412(sh)	1410(sh)	1434	$\nu_aNCC_\alpha C$, $\delta_aCH_3(\alpha,\beta)$
1428	9	15	1396(sh)	1393(25)	1395(sh)	$\delta_sCH_3(\alpha,\beta)$
1410	3	3	1367(56)	1371(31)	1395	$\delta_sCH_3(\alpha)$, $\delta_sC5H_3(\beta)$, ν_sNCC_α
1385	40	4	1350(51)	1355(52)	1350(26)	$\delta_sC1H_3(\beta)$
1300	179	6	1295(56)	1280(61)	1289(19)	δND_2, ν_sCCCN, $\nu C\text{-}CH_3(\alpha)$, $\delta CH_3(\alpha)$
1219	16	3	1196(36)	1206(27)	1193(9)	δND_2, $\delta CC_\alpha C$, $\nu C\text{-}CH_3$
1118	10	0	1108(sh)	1104(13)		δND_2, $\rho CH_3(\alpha,\beta)$
1093	17	7	1075(7)	1070(14)	1068(19)	$\rho CH_3(\alpha,\beta)$, δND_2, $\nu C\text{-}CH_3$
1061	1	0	1038(4)	1044(6)		$\rho CH_3(\alpha,\beta)$
1046	0	0				$\rho CH_3(\alpha,\beta)$
1026	3	0	1010(15)	1009(13)		$\rho CH_3(\alpha,\beta)$
1000	17	1	998(sh)	996(13)		$\rho CH_3(\alpha,\beta)$, δND_2
984	76	5	972(70)	970(38)	975(17)	$\rho CH_3(\alpha,\beta)$, $\nu C\text{-}CH_3$, $\nu C_\alpha\text{-}C_\beta$
889	5	2	877(14)	880(5)	878(15)	δND_2, $\nu C\text{-}CH_3$, $\rho CH_3(\alpha,\beta)$
850	2	0	843(24)	846(6)	835(17)	ρND_2, $\nu C\text{-}CH_3$
682	7	20	658(sh)*	672(9)	680(100)	$\delta OCMe$
669	7	0	648(65)	655(8)		Γ

595	8	4	591(70)	595(10)	592(26)	νN…O, Δ
557	3	1	552(17)	n.m.	546(sh)	Γ
527	16	0	527(sh)			γND_2, $\gamma C\text{-}CH_3$
477	2	2	480(100),490(sh)	n.m.	480(sh)	Δ, $\delta C\text{-}CH_3$, $\delta DNCC_\beta$
			447(50)			?
423	4	5	423(76)	n.m.	423(sh)	Δ, $\delta C\text{-}CH_3(\alpha)$
382	3	5	402(57)	n.m.	399(83)	νN…O, $\delta C\text{-}CH_3$
339	1	0	n.m.			$\delta C\text{-}CH_3(\alpha,\beta)$, Δ
283	0	1	289(76)	n.m.	284(59)	$\gamma C\text{-}CH_3(\alpha)$, $\gamma CC_\alpha C$
263	4	0	n.m.			νN…O, $\delta C\text{-}CH_3$
195	61	0	n.m.			γND_2, $\gamma C\text{-}CH_3$
170	2	0	n.m.			τCH_3
128	7	0	n.m.			$\tau CH_3(\alpha,\beta)$, Γ
120	2	0	n.m.			τCH_3
74	11	0	n.m.			γC-CH3(α,β), γND10
36	3	0	n.m.			τCH_3

[a] See footnote of Table 2.

[b] CH stretching modes of methyl groups at below 3000 cm^{-1} in CCl_4 solution, were overlapped with the mentioned modes of triethylamine.

*, below 700 cm^{-1}obtained with different instrument.

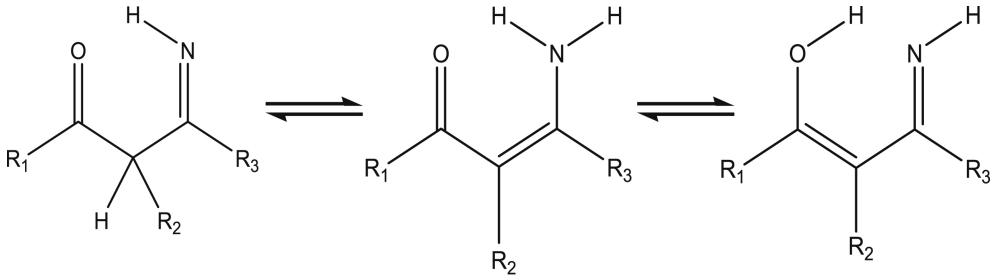

Iminoketone (IK) Aminoketone (AK) Iminoenol (IE)

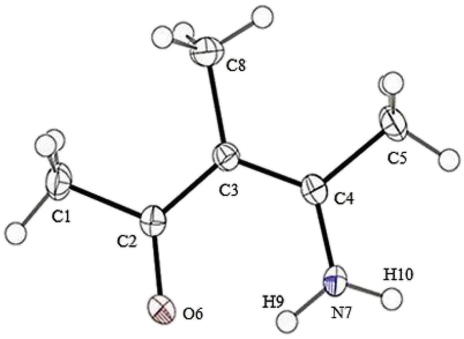

(a)

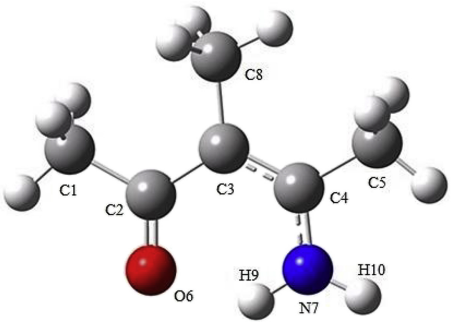

(b)

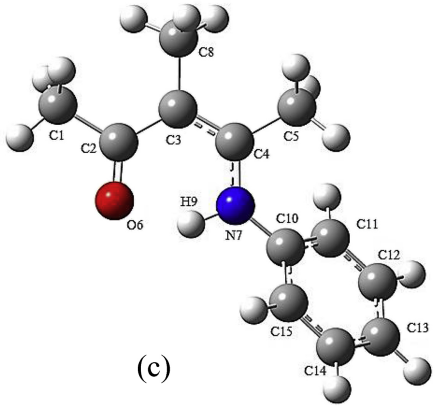

(c)

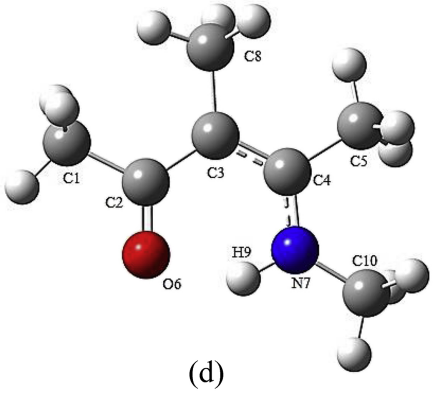

(d)

a

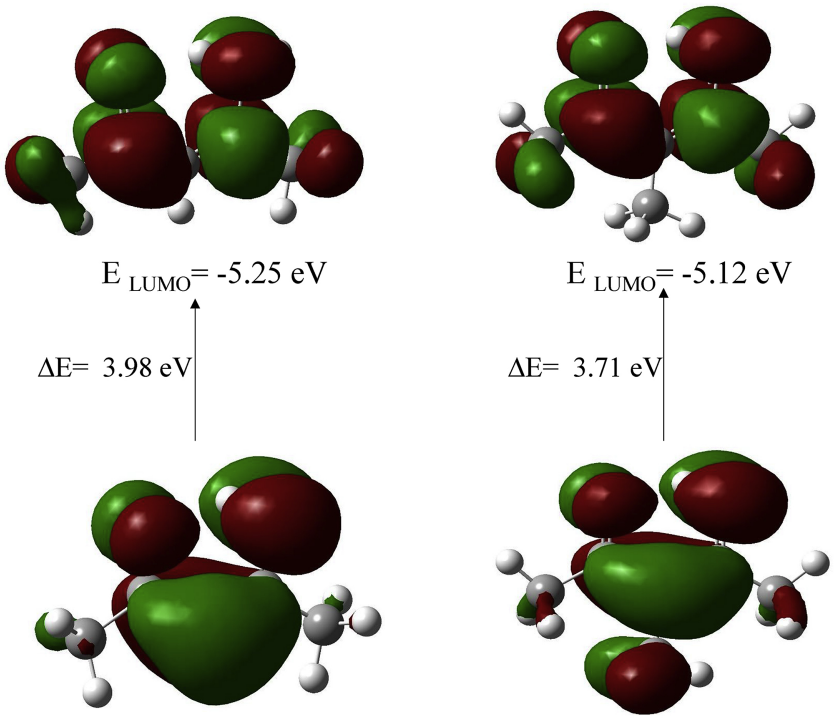
E LUMO= -5.25 eV
ΔE= 3.98 eV
E HOMO= -9.23 eV
APO
E LUMO= -5.12 eV
ΔE= 3.71 eV
E HOMO= -8.83 eV
3-MeAPO

b

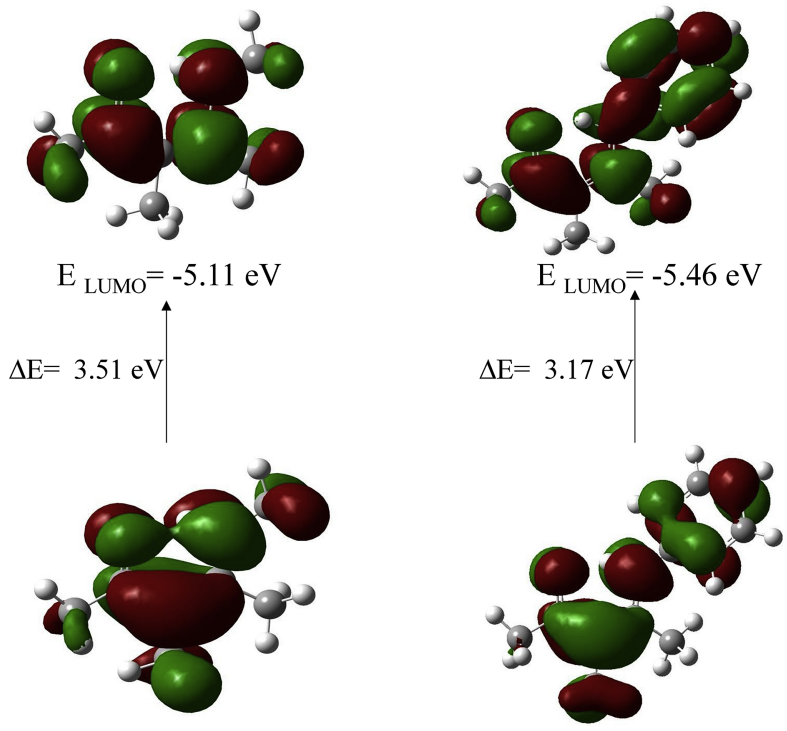
E LUMO= -5.11 eV
ΔE= 3.51 eV
E HOMO= -8.62 eV
3-Me-MeAPO
E LUMO= -5.46 eV
ΔE= 3.17 eV
E HOMO= -8.63 eV
3-Me-PhAPO

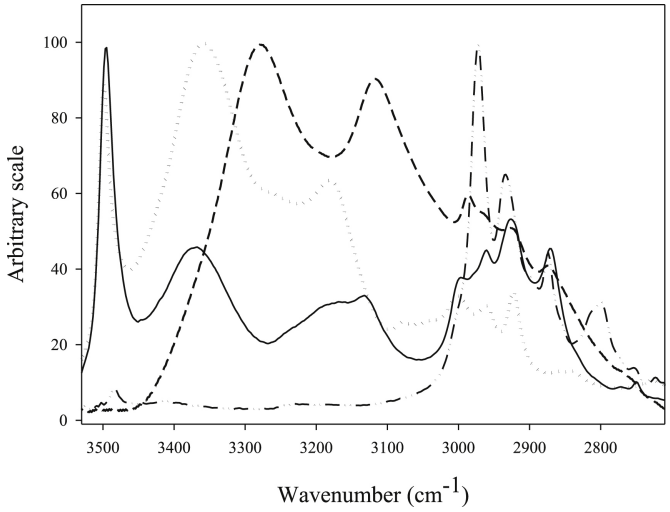

Highlight

- The analysis shows that the keto-amine form is the most stable tautomer.
- All results confirm that the IHB is stronger for 3-MeAPO than for APO.
- N-phenyl substitution leads to a considerably stronger IHB than methyl substitution.
- Complete analysis of vibrational spectra and DFT investigations performed.
- Steric effect is a major factor in increase of IHB strength.